mineral oil bubbler. The cylinder was attached to the vacuum line, evacuated, and then warmed to ambient temperature. Volatile materials were condensed in a −196 °C U-trap while the cylinder was continuously evacuated for at least 24 h. The volatile materials were subsequently separated by high-vacuum fractional condensation. 2,2,2-$(CO)_3$-2-MnB_5H_{10} (**1**) was separated from B_5H_9 and hydrocarbon byproducts by fractional condensation in a −35 °C U-trap. When fractionation was terminated as soon as all of the **1** had distilled into the −35 °C U-trap, most of the unreacted $Mn_2(CO)_{10}$ stayed behind. Multiple fractionations were often required to remove all of the $Mn_2(CO)_{10}$.

Thermolysis of 2-[$(CO)_5Mn$]B_5H_8 (3) and H_2. Two millimoles of **3** was condensed into a 75-mL stainless-steel cylinder equipped with a stainless-steel needle valve. The cylinder was then pressurized with H_2 to 75 atm at ambient temperature and then heated in an oven at 100 °C for 38.5 h. The H_2 pressure at 100 °C was estimated to be ca. 94 atm. Fractionation of the products on a high-vacuum line yielded a mixture of **1** and **3** in a ratio of ca. 1:8 (by ^{11}B NMR). Examination of the nonvolatile solid left in the cylinder indicated decomposition to intractable materials.

Thermolysis of 3 and H_2 with Pt/C. A 75-mL stainless-steel cylinder was loaded with 1.56 g of 5% Pt/C (0.4 mmol of Pt), a needle valve was attached, and the system was evacuated for 18 h. Dry N_2 was admitted, and under N_2, a solution of 1.00 g of **3** (3.9 mmol) in 3 mL of pentane was added by syringe. The cylinder was pressurized with H_2 at ambient temperature to 61 atm. It was then heated at 100 °C for 9.8 days. The H_2 pressure at 100 °C would be ca. 76 atm. After the pressure was released at −196 °C, the volatiles were fractionated on a high-vacuum line, yielding 0.098 g of manganese-containing material in addition to a small amount of $Mn_2(CO)_{10}$. Analysis by ^{11}B NMR showed this to be an approximately equimolar mixture of **1** and **3**. This accounted for less than 15% of the starting manganese.

Reaction of $K[B_5H_{12}]$ with $(CO)_5MnBr$. A procedure developed by Shore et al.[17] was used to prepare 2.0 mmol of $K[B_5H_{12}]$ from $K[B_4H_9]$ and B_2H_6 in 2.7 mL of dimethyl ether. At −78 °C the solvent and excess B_2H_6 were removed by vacuum distillation. After condensation of 3.0 mL of diethyl ether at −196 °C, 0.598 g of $(CO)_5MnBr$ (2.2 mmol) was added under N_2 flow. The system was evacuated, stirred at −78 °C for 1 h and then warmed to ambient temperature over several hours. The ^{11}B NMR spectrum of the diethyl ether solution showed B_5H_9 and smaller amounts of other compounds, which were not identified. No evidence for **1** or **3** was obtained.

Preparation of 2,2,2-$(CO)_3$-2-ReB_5H_{10} (2). Compound **2** was prepared from $Re_2(CO)_{10}$, B_5H_9, and H_2 by using the general procedure for pressurized reactions described above. In each case, 5% Ru/C was used as catalyst. The volatile contents of the cylinder were distilled into the vacuum line during 48 h, and a partial separation was effected by distillation into U-traps cooled to −35 and −196 °C in series. The −196 °C trap contained unreacted B_5H_9, while the −35 °C trap contained a mixture of $B_{10}H_{14}$, 2-[$(CO)_5Re$]B_5H_8, and **2**. Compound **2** was subsequently isolated by condensation in a −10 °C trap.

From a reaction using 5.03 mmol of $Re_2(CO)_{10}$, 25 mmol of B_5H_9, 0.51 mmol of 5% Ru/C, and ca. 100 atm of H_2 at 140–145 °C for 5.8 days was obtained 0.244 g of **2** (0.73 mmol, 7.3% yield based on Re). Another reaction, using 4.22 mmol of $Re_2(CO)_{10}$, 25 mmol of B_5H_9, 0.51 mmol of 5% Ru/C, and ca. 100 atm of H_2 at 120–125 °C for 14 days, gave 0.350 g of **2** (1.05 mmol, 12.4% yield based on Re).

The ^{11}B and ^1H NMR spectra of **2** are tabulated in Tables II and III. The high-resolution mass spectrum of **2** confirmed the molecular formula: calcd for $(^{12}C^{16}O)_3{}^{187}Re^{11}B_4{}^{10}B^1H_{10}$, m/e 335.0661; found, m/e 335.0664.

Reaction of $[(\eta^5\text{-}C_5H_5)Fe(CO)_2]_2$ with B_5H_9 and H_2 over Ru/C. The general procedure for pressurized reactions (described above) was followed by using 0.51 mmol of 5% Ru/C, 5.04 mmol of $[(\eta^5\text{-}C_5H_5)Fe(CO)_2]_2$, and 25 mmol of B_5H_9. With its lower half immersed in liquid nitrogen, the cylinder was pressurized with H_2 to 60 atm. After warming to ambient temperature, it was heated at 142 °C for 6 days. The pressure was released at −196 °C, and the volatile contents of the cylinder were removed by vacuum distillation as it was warmed to ambient temperature. A small amount of yellow-brown solid was isolated by condensation in a −35 °C U-trap. This material was identified by ^{11}B NMR as impure 2-$(\eta^5\text{-}C_5H_5)$-2-FeB_5H_{10}.[8a] More of this compound was obtained by extraction of the solid residue remaining in the cylinder with CH_2Cl_2. The total amount of 2-$(\eta^5\text{-}C_5H_5)$-2-FeB_5H_{10} obtained was small and was not measured.

Acknowledgment. This work was supported in part by research grants and departmental instrumentation grants from the National Science Foundation.

Registry No. **1**, 71230-48-3; **2**, 98586-75-5; **3**, 98586-76-6; $Mn_2(CO)_{10}$, 10170-69-1; B_5H_9, 19624-22-7; $K[B_5H_{12}]$, 11056-98-7; $(CO)_5MnBr$, 14516-54-2; $Re_2(CO)_{10}$, 14285-68-8; $[(\eta^5\text{-}C_5H_5)Fe(CO)_2]_2$, 12154-95-9; 2-$(\eta^5\text{-}C_5H_5)$-2-$FeB_5H_{10}$, 71661-61-5.

Supplementary Material Available: Figures 2 and 3, showing the ^{11}B and ^2H NMR spectra of 2,2,2-$(CO)_3$-2-ReB_5H_{10} (2 pages). Ordering information is given on any current masthead page.

Contribution from the Department of Chemistry,
The Ohio State University, Columbus, Ohio 43210

Electrocatalysis of Oxygen Reduction. 5. Oxygen to Hydrogen Peroxide Conversion by Cobalt(II) Tetrakis(*N*-methyl-4-pyridyl)porphyrin

RAY J. H. CHAN, Y. OLIVER SU, and THEODORE KUWANA*

Received November 27, 1984

Cobalt(III) tetrakis(*N*-methyl-4-pyridyl)porphyrin (abbreviated $Co^{III}TMPyP$), although water soluble, adsorbs irreversibly on the surface of a highly polished glassy-carbon electrode. This porphyrin readily undergoes a one-electron reduction, either in solution or adsorbed, to produce the cobaltous form, which catalyzes the reduction of oxygen quantitatively to hydrogen peroxide. The pK_{a_1} of $Co^{III}TMPyP$ is found to shift from a value of 6.0 for the solution to 2.0 for the adsorbed case. Thus, the electrode potential at which oxygen catalysis occurs is dependent on the pH and on the concentration ratio of the solution cobalt porphyrin to oxygen. However, at a pH of ca. 4 the redox potential of the solution CoTMPyP becomes more positive in value than that of the reversible O_2/H_2O_2 potential so that the electrogenerated cobaltous porphyrin no longer catalyzes the reduction of oxygen. The potential of catalysis then shifts negatively to the adsorbed CoTMPyP, which, upon reduction, converts the O_2 to H_2O_2. The addition of thiocyanate ion to the solution can accelerate the rate of electron transfer from the electrode to the cobalt porphyrin. This addition, in low concentrations, can favorably affect the potential at which oxygen is catalytically reacted by decreasing the overpotential for the $Co^{III}TMPyP$ reduction.

Introduction

Of numerous studies[1-31] on the electrocatalysis of dioxygen with monomeric metal macrocyclic complexes, our laboratory has concentrated on water-soluble iron[19-25] and cobalt[26-28] porphyrins (abbreviated FeP and CoP or $PCo^{II,III}$) and the elucidation of their catalytic mechanism for dioxygen reduction at glassy-carbon

* To whom correspondence should be addressed at the Center for Bioanalytical Research, West Campus, The University of Kansas, Lawrence, KS 66046.

(1) Jasinski, R. J. *J. Electrochem. Soc.* **1965**, *112*, 526.
(2) Jasinski, R. J. *Nature (London)* **1964**, *201*, 1212.
(3) Appleby, A. J.; Savy, M. *Proc.—Electrochem. Soc.* **1977**, *77-6*, 321.
(4) Appleby, A. J.; Savy M. *J. Electroanal. Chem. Interfacial Electrochem.* **1980**, *111*, 91.
(5) Appleby, A. J.; Savy, M. *Electrochim. Acta* **1976**, *21*, 576.

0020-1669/85/1324-3777$01.50/0

electrodes (GCE's). For example, with the water-soluble iron tetrakis(*N*-methyl-4-pyridyl)porphyrin (abbreviated FeTMPyP), the electrogenerated ferrous porphyrin catalyzed the reduction of both dioxygen and hydrogen peroxide via an "EC" reaction sequence

I. "E" step

$$Fe^{III}TMPyP + e^- = Fe^{II}TMPyP \quad (1)$$

II. "C" steps

$$2Fe^{II}TMPyP + O_2 + 2H^+ = 2Fe^{III}TMPyP + H_2O_2 \quad (2)$$

$$2Fe^{II}TMPyP + H_2O_2 + 2H^+ = 2Fe^{III}TMPyP + 2H_2O \quad (3)$$

where reactions 2 and 3 were written to reflect the stoichiometry of the O_2 and H_2O_2 reductions. The experimental and computer-simulated cyclic voltammograms (CV's) were consistent with this mechanism. In the simulation, only one rate-limiting step was assumed to be present in each of reactions 2 and 3. If the initial step of the $Fe^{II}TMPyP$ reaction with O_2 or H_2O_2 is rate limiting, the second electron for the reduction of any intermediate states can come either from the electrode or, as written in reactions 2 and 3, from another $Fe^{II}TMPyP$. If the rates of such follow-up reactions are rapid,[24,25] the potential of the catalysis corresponds closely to the redox potential of reaction 1, the "E" step. There was no evidence that this iron porphyrin adsorbed on the surface of a highly polished GCE, at least when sulfuric acid or phosphate buffer solutions were employed.

In sharp contrast to the iron case, the cobalt analogue, CoTMPyP, adsorbs irreversibly onto a highly polished GCE surface and catalyzes O_2 reduction to H_2O_2 (>90% efficiency). The reduction of $Co^{III}TMPyP$ to $Co^{II}TMPyP$[26-28] governs the potential for catalysis. The water solubility of CoTMPyP provides an unique opportunity to compare the adsorbed vs. the solution electrochemical properties of this porphyrin (or of the unmethylated cobalt tetrakis(4-pyridyl)porphyrin, CoTPyP) in the absence and presence of oxygen particularly as a function of pH. Such a comparison is particularly significant since there has been a question of whether the surface adsorption alters the properties of a metal complex. Correlation of information from the homogeneous electrochemistry with the known solution chemistry, as demonstrated with FeTMPyP, should assist in the design of experiments to delineate the thermodynamic and kinetic parameters. For example, it has been reported by Pasternack et al.[32-37] that thiocyanate ion, SCN^-, can complex with CoTMPyP and accelerate the homogeneous electron-exchange reactions. Such an acceleration also occurs with the heterogeneous electron transfer with $Co^{III}TMPyP$, affecting the potential of oxygen catalysis, as will be discussed herein.

To set the status of oxygen catalysis via metal macrocyclic complexes into perspective, a brief informational discussion is pertinent. It now appears that there are two distinct types of complexes for oxygen catalysis. These can be classified according to the correspondence between the potential for catalysis and the redox potential of the complex or according to the extent of catalysis: i.e., whether oxygen is reduced to hydrogen peroxide or to water. A close correspondence in potential occurs when the "C" step(s) is sufficiently rapid that the potential of the electrode reaction is determined by the reduction of the macrocyclic complex rather than by any intermediate(s) formed between the reduced state of the complex and oxygen. Such is the case with FeTMPyP. The ferrous porphyrin complexes are capable of reducing both oxygen and hydrogen peroxide while the cobaltous porphyrins reduce oxygen rapidly only to hydrogen peroxide. These cases of CoDTDP, CoTPP, and CoTSPc differ from the "EC" case, since an intermediate-state species, rather than the macrocycle, reacts and determines the potential of the electrode.

Durand and Anson[29] have reported that adsorbed cobalt(II) 3,13-(diethylacetoxy)-2,7,12,17-tetramethyl-3,13-diethylporphyrin (abbreviated CoDTDP) on pyrolytic graphite catalyzed the conversion of oxygen to hydrogen peroxide at potentials several hundred millivolts more negative than that of the $Co^{III/II}DTMP$ redox reaction (pH 1–14). The reported formal potential, $E^{\circ\prime}$ = +0.79 V (vs. NHE), of this couple in 1 M CF_3COOH is more positive than that of other cobalt porphyrins. A close analogue, cobalt(II) etioporphyrin, has a formal potential of +0.54 V with the ring oxidation occurring at +1.18 V. In spite of this difference, oxygen catalysis occurred at +0.44 V, close to that of CoTMPyP. The reaction sequence proposed was (e.g., at pH >7)

$$PCo^{II} + O_2 = PCo^{II}O_2 \quad \text{rate-determining step} \quad (4)$$

$$PCo^{II}O_2 + H^+ = PCo^{II}O_2H^+ \quad (5)$$

$$PCo^{II}O_2H^+ + 2e^- = PCo^{II}O_2H^- \quad (6)$$

$$PCo^{II}O_2H^- = PCo^{II} + O_2H^- \quad (7)$$

where the electrode reaction involved an oxygen–CoP intermediate species and the cobalt remained mainly in the reduced cobaltous state. For the case of cobalt tetraphenylporphyrin (abbreviated CoTPP), Buttry and Anson[31] proposed $Co^{III}TPP(O_2^-)$ as the intermediate.

Zagal, Bindra, and Yeager[9,11] studied the O_2 catalytic reduction by the adsorbed Co(II) tetrasulfonated phthalocyanine (abbreviated $Co^{II}TSPc$). The potential for catalysis was more negative than that of the Co(III/II) redox couple by ca. 1.1 V in 0.05 M H_2SO_4. In their proposed mechanism, the rate-determining step was an electron-transfer reaction involving an oxygenated intermediate.

(6) Kozawa, A.; Zilionis, V. E.; Brodd, R. J. *J. Electrochem. Soc.* **1970**, *117*, 1474.
(7) Kozawa, A.; Zilionis, V. E.; Brodd, R. J. *J. Electrochem. Soc.* **1971**, *118*, 1705.
(8) Radin, J. P. *Electrochim. Acta* **1974**, *19*, 83.
(9) Zagal, J.; Sen, R. K.; Yeager, E. B. *J. Electroanal. Chem. Interfacial Electrochem.* **1977**, *83*, 207.
(10) Sen, R. K.; Zagal, J.; Yeager, E. B. *Inorg. Chem.* **1977**, *16*, 3379.
(11) Zagal, J.; Bindra, P.; Yeager, E. B. *J. Electrochem. Soc.* **1980**, *127*, 1506.
(12) Van Den Brink, F.; Barendrecht, E.; Visscher, W. *Recl. Trav. Chim. Pays-Bas* **1980**, *99*, 253.
(13) Van Veen, J. A. R.; Visser, C. *Electrochim. Acta* **1979**, *24*, 921.
(14) Van Veen, J. A. R.; Van Baar, J. F.; Kroese, K. J.; Collegem, J. G. F.; de Wit, N.; Colign, H. A. *Ber. Bunsen-Ges. Phys. Chem.* **1981**, *85*, 693.
(15) Van Veen, J. A. R.; van Barr, J. F.; Kroese, K. J. *J. Chem. Soc., Faraday Trans. 1* **1981**, *77*, 2827.
(16) Schiffrin, J. "Electrochemistry"; The Royal Society of Chemistry: London, 1983; Chapter 4.
(17) Jones, R. D.; Summerville, D. A.; Basolo, F. *Chem. Rev.* **1979**, *79*, 139.
(18) Jahnke, H.; Schonbron, M.; Zimmerman, G. *Top. Curr. Chem.* **1976**, *61*, 133.
(19) Kuwana, T.; Fujihara, M.; Sanakawa, K.; Osa, T. *J. Electroanal. Chem. Interfacial Electrochem.* **1978**, *88*, 299.
(20) Bettelheim, A.; Kuwana, T. *Anal. Chem.* **1979**, *51*, 2257.
(21) Bettelheim, A.; Chan, R. J. H.; Kuwana, T. *J. Electroanal. Chem. Interfacial Electrochem.* **1980**, *110*, 93.
(22) Kobayashi, N.; Fujihira, M.; Osa, T.; Kuwana, T. *Bull. Chem. Soc. Jpn.* **1980**, *53*, 2195.
(23) Forshey, P. A.; Kuwana, T. *Inorg. Chem.* **1981**, *20*, 693.
(24) Dimarco, D. M.; Forshey, P. A.; Kuwana, T. *ACS Symp. Ser.* **1982**, *No. 192*, 72.
(25) Forshey, P. A.; Kuwana, T. *Inorg. Chem.* **1983**, *22*, 699.
(26) Bettelheim, A.; Chan, R. J. H.; Kuwana, T. *J. Electroanal. Chem. Interfacial Electrochem.* **1979**, *99*, 390.
(27) Chan, R. J. H. Ph.D. Thesis, The Ohio State University, 1982.
(28) Chan, R. J. H.; Ueda, C.; Kuwana, T. *J. Am. Chem. Soc.* **1983**, *105*, 3713.
(29) Durand, R. R., Jr.; Anson, F. C. *J. Electroanal. Chem. Interfacial Electrochem.* **1982**, *134*, 273.
(30) Shigehara, K.; Anson, F. C. *J. Phys. Chem.* **1982**, *86*, 2776.
(31) Buttry, D. A.; Anson, F. C. *J. Am. Chem. Soc.* **1984**, *106*, 59.
(32) Pasternack, R. F.; Cobb, M. A. *Biochem. Biophys. Res. Commun.* **1973**, *51*, 507.
(33) Pasternack, R. F.; Cobb, M. A. *J. Inorg. Nucl. Chem.* **1973**, *35*, 4327.
(34) Pasternack, R. F.; Spiro, E. G.; Teach, M. *J. Inorg. Nucl. Chem.* **1975**, *36*, 599.
(35) Pasternack, R. F.; Cobb, M. A.; Sutin, N. *Inorg. Chem.* **1975**, *14*, 866.
(36) Pasternack, R. F.; Sutin, N. *Inorg. Chem.* **1974**, *13*, 1956.
(37) Pasternack, R. F. *Inorg. Chem.* **1976**, *15*, 643.

Table I. Spectral Data

compd	soln conditions	λ, nm	ε, M^{-1} cm^{-1}
$Co^{III}TMPyP(H_2O)_2$	0.1 N H_2SO_4	433	2.14×10^5
		543	1.60×10^4
	pH 2[33]	434	2.14×10^5
$Co^{II}TMPyP(H_2O)_2$	0.1 N H_2SO_4	427	1.38×10^5
		536	1.33×10^4
$Co^{III}TMPyP(H_2O)(OH^-)$	pH 8.0	436	1.66×10^5
		547	1.56×10^4
	pH 8[33]	437	1.68×10^5
$Co^{III}TMPyP(OH^-)_2$	pH 11.5[33]	445	1.41×10^5
$Co^{III}TMPyP(H_2O)(SCN^-)$	pH 2[33]	438	1.86×10^5
$Co^{III}TPyP(H_2O)_2$	0.1 N H_2SO_4	430	2.14×10^5
		542	1.53×10^4
$Co^{II}TPyP(H_2O)_2$	0.1 N H_2SO_4	424	1.46×10^5
		535	1.43×10^4

Geiger and Anson[38] have described an interesting case of oxygen to hydrogen peroxide catalysis with the macrocyclic cobalt complex, *trans*-$[Co([14]aneN4)(OH_2)_2]^{3+}$. Although their catalysis was observed to occur close to the potential of the III/II redox couple, two different intermediates can be formed depending on the ratio of the concentration of the macrocycle to that of oxygen. These intermediates were then electrochemically reduced at more negative potentials to release hydrogen peroxide.

To further characterize the catalysis of O_2 reduction, this paper describes the detailed electrochemistry of the solution phase and of surface-adsorbed $Co^{III}TMPyP$ (which applies to CoTPyP as well) in the presence and absence of oxygen. Also, the effects of pH and thiocyanate ion on both the electrochemistry and the O_2 catalysis are examined to assess the electron-transfer mechanisms of these two cobalt porphyrins. The experimental approach depends extensively on the coupling of optical and electrochemical methods, as illustrated previously in our study of $Fe^{III}TMPyP$.[23,25]

Experimental Section

CoTMPyP was synthesized by two different procedures, a and b:

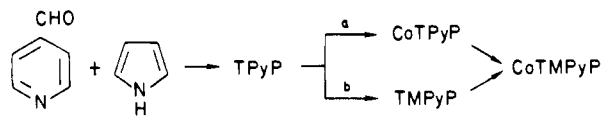

The tetrapyridylporphyrin (TPyP) was initially synthesized with use of Adler's method.[27] In procedure a, TPyP was metalated by refluxing in DMF with $CoCl_2$ followed by Soxhlet extraction of the unmetalated TPyP with methanol. The CoTPyP was then methylated in neat dimethyl sulfate. Alternatively, in procedure b, TPyP was methylated prior to metalation. The CoTMPyP was precipitated as the perchlorate salt by the dropwise addition of saturated $NaClO_4$. The precipitate was recrystallized from distilled water. Infrared, proton NMR, and UV–visible spectral data were used to verify product composition and purity.

To compare the extent of methylation of CoTMPyP and CoTPyP, infrared spectra were obtained on a Perkin-Elmer Model 337 spectrophotometer with KBr pellets. The C=N stretching band of pyridine at 1595 cm^{-1} shifted to 1647 cm^{-1} on methylation. Proton NMR spectra were obtained on a Varian EM 90-MHz instrument with chemical shifts reported relative to an internal Me_4Si standard in Me_2SO-d_6 (δ 9.37 (s, 8 H), 9.27 (d, 8 H), 8.92 (d, 8 H), 4.80 (s, 12 H)). The results indicate the expected stoichiometric ratio of protons on the porphyrin ring and show no impurity peaks. The UV–visible spectral data, obtained with a Cary Model 15 spectrophotometer, are listed and compared with literature values in Table I. Molar absorptivities for the reduced product, $Co^{II}TMPyP$, were determined from spectra taken with an optically transparent thin-layer electrode (OTTLE) cell in which known amounts of $Co^{III}TMPyP$ were electroreduced. The infrared, NMR, and UV–visible spectroscopic data indicate less than 1% impurities in the CoTMPyP samples.

All chemical reagents were analytical grade, and solutions were prepared with doubly distilled water. Solution pHs were determined with a Corning Model 7 pH meter equipped with a Sargent-Welch combination glass pH electrode (Model S-30070-10). Prepurified nitrogen (99.99%) was used for deoxygenation. Oxygen concentrations in air-saturated solutions were assumed to be 0.24 mM at 20 ± 1 °C. The concentrations of $Co^{III}TMPyP$ solutions were determined by spectroscopic measurements at λ = 433 nm in 0.1 N H_2SO_4.

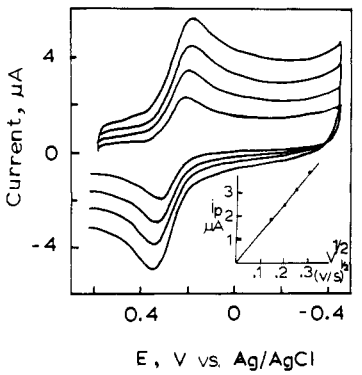

Figure 1. Cyclic voltammograms of 2.6×10^{-4} M CoTMPyP in 0.1 N H_2SO_4 at scan rates of 20, 40, 62.5, and 90 mV/s (area of GCE 0.144 cm^2). Oxygen was removed by N_2 degassing. Inset: plot of i_p vs. $v^{1/2}$.

Cyclic voltammetry (CV), chronoamperometry, and chronocoulometry were conducted with an all-glass, three-electrode cell. The working electrodes were glassy carbon, either from Tokai Carbon Co., Tokyo (grades GC-20 or GC-30), or from BAS (Bioanalytical Systems, Inc., West Lafayette, IN). These were polished consecutively with 1.0-, 0.3-, and 0.05-μm alumina on an optical flat until a mirrorlike finish was obtained. The polished electrode was cleaned in an ultrasonic water bath for 5 min to remove surface alumina and carbon particles. The polishing procedure was repeated if the electrode was not used immediately. A Pt wire served as the auxiliary electrode and was isolated from the main working compartment by a medium-porosity glass frit. A reference Ag/AgCl (saturated KCl) electrode was employed for all voltammetric experiments.

CV experiments were performed with a BAS Model CV-1A potentiostat with Houston (Houston Instrument Co., Austin, TX) Model 2000 X-Y recorder. A PAR (Princeton Applied Research Corp., Princeton, NJ) Model 174A polarographic analyzer with a Model 175 universal programmer served for the chronoamperometric and chronocoulometric experiments. Spectroelectrochemistry was conducted with an Au minigrid in an OTTLE cell with the optical path length (0.022 cm) being determined with known solutions of ferricyanide (ε = 1020 M^{-1} cm^{-1} at a wavelength of 418 nm).

Coulometric experiments were conducted with a carbon electrode in a thin-layer configuration that had a cell volume of 6.6 μL, as determined from the reduction of known solutions of ferricyanide. For macroscale coulometry, a large Tokai glassy-carbon electrode (area 11.4 cm^2) served as the working electrode and a Pt wire in a coil configuration as the auxiliary electrode in a two-compartment cell, the compartments being separated by a NaFion (Du Pont) membrane. The potential of the working electrode vs. a Ag/AgCl reference was controlled by a BAS Model SP-2 potentiostat. The electrochemical charge was determined by integrating the area under the recorded current–time curves.

Results and Discussion

1. Electrochemical Parameters of CoTMPyP in the Absence of Oxygen. Typical cyclic voltammograms (CV's) of $Co^{III}TMPyP$ in 0.1 N H_2SO_4 solution, in the absence of O_2 at a highly polished GCE, are shown as a function of the scan rate in Figure 1. The separation of the peak currents indicates that the electrode reaction is quasi-reversible. However, the degree of reversibility was quite dependent on the history and surface pretreatment of the GCE. Thus, the heterogeneous rate constant, k_s, varied between 5×10^{-3} and 1.0×10^{-4} cm s^{-1} for $Co^{III}TMPyP$ in H_2SO_4 solutions, as determined from CV data by the method of Nicholson and Shain.[39] The peak currents, i_p's, were diffusion limited, with the plots of i_p vs. square root of scan rate being linear over a 10-fold scan range. $E^{\circ\prime}$ (assumed equivalent to the average of E_{pc} and E_{pa}) was 0.41 ± 0.01 V (vs. NHE) in good agreement with values (0.415 and 0.42 V) determined spectroelectrochemically in an OTTLE cell.[40] The electrochemical parameters of formal potential, $E^{\circ\prime}$, the number of electrons, n, transferred per CoP, and the diffusion coefficient, D, are summarized in Table II. The n value of unity

(38) Geiger, T.; Anson, F. *J. Am. Chem. Soc.* **1981**, *103*, 7489.

(39) Nicholson, R. S.; Shain, I. *Anal. Chem.* **1964**, *36*, 706.

(40) Rohrbach, D. F.; Deutsch, E.; Heineman, W. R.; Pasternack, R. F. *Inorg. Chem.* **1977**, *16*, 2650.

Table II. Electrochemical Data of $Co^{III}TMPyP$

A. $E^{\circ\prime}$ Values[d]

soln conditions	$E^{\circ\prime}$, V (vs. NHE)	method (ref)[a]
0.1 N H_2SO_4	+0.415	OTTLE cell (40)
0.1 N H_2SO_4	+0.42 (±0.01)	OTTLE cell
pH 1–5	+0.41 (±0.01)	CV, $^1/_2(E_{pa} + E_{pc})$

B. Thin-Layer Coulometric Determination of n Values[b]

$[Co^{III}TMPyP]$, M	soln	total Q, mC	n
5.93×10^{-4}	0.1 N H_2SO_4	0.636	0.95
2.06×10^{-3}	0.1 N H_2SO_4	1.34	1.04
1.13×10^{-3}	pH 7.0	0.594	0.85
			0.94 ± 0.11 (av)

C. Values of Diffusion Coefficient

soln	10^6D, $cm^2\ s^{-1}$	method[c]
$[Co^{III}TMPyP]$ =	2.1 ± 0.3	chronoamperometry
3×10^{-4}–1×10^{-3} M	2.3 ± 0.3	
in 0.1 N H_2SO_4	2.0 ± 0.3	
	1.9 ± 0.4	
	2.4 ± 0.1	
	2.5 ± 0.1	RDE
	2.2 (av) (s = 0.24)	

[a] If no reference given, data obtained in present study. [b] Exhaustive electrolysis with the applied potential stepped from +0.7 to 0.0 V; cell volume 6.6 μL. [c] Chronoamperometry with highly polished glassy-carbon electrode with area of 0.07 cm^2; RDE also GCE with area of 0.755 cm^2; applied potential stepped from +0.7 to 0.0 V. [d] n = 1 in all cases.

was verified by the exhaustive electrolysis of $Co^{III}TMPyP$ solutions in a thin-layer cell. The diffusion coefficient was determined via chronoamperometric and rotating-disk electrode experiments to be 2.2 (s = 0.24) × 10^{-6} $cm^2\ s^{-1}$. This compares closely to a value of 2.5 (±0.01) × 10^{-6} $cm^2\ s^{-1}$ from chronocoulometry data.[23] The electrode reaction is

$$Co^{III}TMPyP + e^- = Co^{II}TMPyP \quad (8)$$

where the assignment of the reduction to the metal center was based on UV–visible and ESR results, similar to the case of cobalt tetraphenylporphyrin (abbreviated CoTPP). Also if the TMPyP were unmetalated, a quasi-reversible two-electron reduction would be observed with an $E^{\circ\prime}$ = +0.13 V and an irreversible multi-electron reduction at ca. −0.40 V.[23] Finally, only the metalated complex catalyzed oxygen reduction; the nonmetalated TMPyP exhibited no such catalytic activity.

Pasternack et al.[32-37] have extensively studied the homogeneous solution chemistry of $Co^{III}TMPyP$. They have reported that this porphyrin was diamagnetic and low spin, whereas, in contrast, the $Fe^{III}TMPyP$ is paramagnetic and high spin. Also, $Co^{III}TMPyP$ has only a single absorbance peak in the Soret region while $Fe^{III}TMPyP$ has two peaks. Pasternack and Cobb[32,33] have determined two pK_a values from the analysis of photometric titration data; pK_{a_1} = 6.0 and pK_{a_2} = 10.0. Using the conditions of their experiment with 4.34×10^{-6} M $Co^{III}TMPyP$ and with a Simplex computer analysis[27] of the absorbance change at the wavelength maximum of 430 nm ($\epsilon_{430} = 2.11 \times 10^5\ M^{-1}\ cm^{-1}$), we obtained values of pK_{a_1} = 5.9 ± 0.1 and pK_{a_2} = 9.9 ± 0.1. The acid–base equilibria are

$$Co^{III}TMPyP(H_2O)_2^{5+} = Co^{III}TMPyP(H_2O)(OH^-)^{4+} + H^+ \quad (9)$$

$$Co^{III}TMPyP(H_2O)(OH^-)^{4+} = Co^{III}TMPyP(OH^-)_2^{3+} + H^+ \quad (10)$$

Thus, the two axial positions of the six-coordinate CoP complex are assumed to be occupied by water in a noncomplexing, acidic media.

The above acid–base results are consistent with the CV's in the pH range of 1–10. $E^{\circ\prime}$ vs. pH is plotted in Figure 2, trace a. As seen in this trace, the $E^{\circ\prime}$ is independent of pH in the acidic region

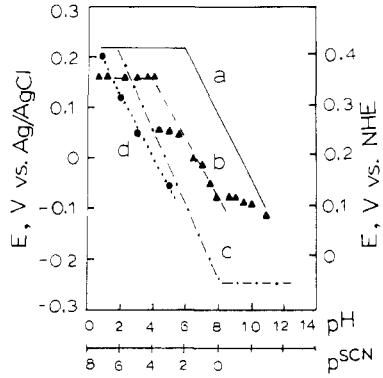

Figure 2. Various potentials plotted vs. pH or pSCN: (a) Formal potential, $E^{\circ\prime}$, vs. pH for solution $Co^{III/II}TMPyP$ without oxygen; (b) $E_{p,cat}$ vs. pH for 2.7×10^{-4} M CoTMPyP in air-saturated solutions (solid triangles are data points); (c) E_p and $E_{p,cat}$ for adsorbed CoTMPyP in the absence and presence of oxygen, respectively; (d) $E_{p,cat}$ vs. pSCN (lower scale) for adsorbed CoTMPyP in air-saturated 0.1 N H_2SO_4 with SCN^- added (solid circles are data points).

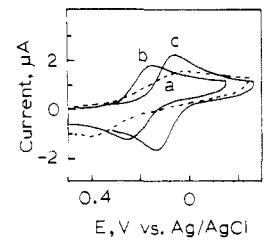

Figure 3. Cyclic voltammograms of 5.0×10^{-4} M CoTMPyP with various concentrations of SCN^- (electrode area 0.070 cm^2, scan rate 40 mV/s): (a) 0.0; (b) 2.0×10^{-4}; (c) 3.0×10^{-3} M.

and then decreases with a slope of 60 mV/pH unit at pH values greater than 6. The "break" at pH 6 corresponds to pK_{a_1}. Because the CV's became less well defined at pH greater than ca. 10, no attempt was made to delineate the value of pK_{a_2} from CV data. In contrast to $Fe^{III}TMPyP$, there were no other "breaks" in the $E^{\circ\prime}$ vs. pH, which indicated a pK_a for the reduced, *cobaltous* form of the complex. Thus, the electrode reaction at pH >6 is

$$Co^{III}TMPyP(H_2O)(OH^-) + e^- + H^+ = Co^{II}TMPyP(H_2O) + H_2O \quad (11)$$

The product of the reduction throughout the entire pH range studied is *cobaltous porphyrin with both axial positions occupied by water*. Further confirmation of the reduced state configuration, being independent of pH, was the one-to-one correspondence of UV–vis absorption spectra from solutions of $Co^{II}TMPyP$ at different pH values produced by the exhaustive electroreduction of $Co^{III}TMPyP$ in an OTTLE cell.

2. Effect of Thiocyanate Ion. Pasternack et al.[34-37] reported that chloride and thiocyanate anions catalyzed various homogeneous reductions of $Co^{III}TMPyP$. For example, $Co^{III}TMPyP(H_2O)(SCN^-)$ was reduced 10 times faster than $Co^{III}TMPyP(H_2O)_2$ by $Ru^{II}(NH_3)_6$ in a chloride ligand medium. The axial ligand effect was rationalized thermodynamically by assuming that the thiocyanate complex could be reduced more easily than $Co^{III}TMPyP$ by ca. 0.12 V. This conclusion led to a suggestion that the bonding was Co–SCN rather than Co–NCS.[35,36] We believe, however, that the shift of 0.12 V is due to the effect of SCN^- to the kinetics and not the thermodynamics of the electron-transfer reaction.

As mentioned, the electrochemistry of $Co^{III}TMPyP$ is very sensitive to the state of the GCE surface. Occasionally, an electrode exhibited sufficient irreversibility that the CV peaks were very broad with E_p's of 200–400 mV. Thus, the addition of SCN^- ligand had a dramatic effect on the $Co^{III}TMPyP$ electrochemistry in such cases, as illustrated by the CV's shown in Figure 3. Trace a appears irreversible for 5.0×10^{-4} M $Co^{III}TMPyP$ in 0.1 N H_2SO_4 solution. Traces b and c, obtained with the same GCE,

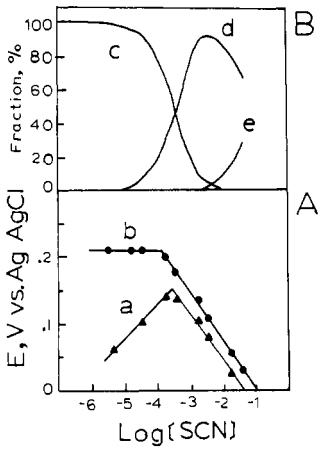

Figure 4. (A) Plot of $^1/_2(E_{pc} + E_{pa})$ and E_{pc} of CoTMPyP–SCN vs. log [SCN^-]: (a) E_{pc}; (b) $^1/_2(E_{pc} + E_{pa})$. (B) Fraction distribution of CoTMPyP complexes: (c) $Co^{III}TMPyP(H_2O)_2$; (d) $Co^{III}TMPyP(H_2O)(SCN^-)$; (e) $Co^{III}TMPyP(SCN^-)_2$.

show increased reversibility when 2.0×10^{-4} and 3.0×10^{-3} M SCN^- were added. When small increments of SCN^- were added, the E_{pc} initially shifted in a positive direction. Then, as the SCN^- concentration nearly equaled that of $Co^{III}TMPyP$, the E_{pc}'s shifted in a negative direction (see plot of E_{pc} vs. log [SCN^-] in Figure 4A, curve a). The initial shift in the E_{pc} is due to the effect of SCN^- on the kinetics of the electron transfer to $Co^{III}TMPyP$. However, if the formal potential, $E°'$, which is determined from $(E_{pa} + E_{pc})/2$, is plotted as a function of SCN^- concentration, curve b results. This curve reflects the thermodynamics of $Co^{III/II}TMPyP$ in the presence of SCN^-. That is, at low concentrations, $E°'$ is independent of [SCN^-] until a pSCN which corresponds to the value of pK_{f_1} (K_{f_1} = first formation constant of the mono(thiocyanate) complex) is reached. At [SCN^-] > ca. 3×10^{-4} M, the $E°'$ vs. log [SCN^-] plot has a 60-mV slope due to the reaction

$$Co^{III}TMPyP(H_2O)(SCN^-)^{4+} + e^- = Co^{II}TMPyP(H_2O)^{4+} + SCN^- \quad (12)$$

The "break" in the curve occurs, of course, at the value of pK_{f_1}. This formation constant was determined to be 6.5 (±0.1) × 10^3 M^{-1} by a "best fit" computer analysis of the optical absorbance change at 430 nm during a SCN^- titration of a 2.95×10^{-5} M $Co^{III}TMPyP$ solution in H_2SO_4. Two isosbestic points were observed at wavelengths of 441 and 449 nm during the titration; the second isosbestic point appeared when the SCN^- concentration became greater than 0.05 M and was analyzed as being due to the second formation constant, K_{f_2}, with a value of 12 ± 2 M^{-1}. These K_f values are in excellent agreement with those previously reported.[32,33] With use of these K_f values, the species distribution was computer calculated for a $Co^{III}TMPyP$–SCN solution and the results are shown in Figure 4B. This distribution is plotted as a fractional concentration vs. log [SCN^-] in Figure 4B and nicely explains curve b of Figure 4A.

The shape of curve b in Figure 4A is a composite of the kinetic and the thermodynamic effects to the E_{pc}, as a function of SCN^- concentration. The initial irreversibility of $Co^{III}TMPyP$ on the GCE will determine where the "break" will occur in this curve. As stated previously, the k_s value fluctuated between 5×10^{-3} and 1×10^{-4} cm s^{-1}. However, it increased to greater than 2×10^{-2} cm s^{-1} in the presence of a 100-fold excess of SCN^- to $Co^{III}TMPyP$.

The product of reaction 12 is proposed to be the cobaltous form without any thiocyanate ligand. The electrochemical reduction (E_{appl} = −0.2 V) of a thoroughly degassed solution of 1.38×10^{-4} M $Co^{III}TMPyP$ in the presence of 2.5×10^{-3} M SCN^- in an OTTLE cell produced only the spectrum of $Co^{II}TMPyP(H_2O)$ with a characteristic λ_{max} of 428 nm. However, Pasternack[35] had proposed that the cobaltous form retained thiocyanate as a ligand due to the Soret band of $Co^{III}TMPyP(H_2O)(SCN^-)$ being shifted from 438 to 434 nm upon reduction of a solution containing 8 × 10^{-3} M SCN^- (89% of $Co^{III}TMPyP$ present as the mono(thiocyanato) complex) by $Ru^{II}(NH_3)_6$. The reason for this discrepancy is unknown.

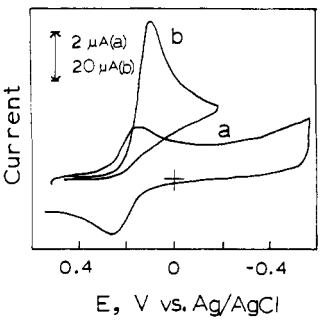

Figure 5. Cyclic voltammograms of 2.69×10^{-4} M CoTMPyP under N_2 and O_2 in 0.1 N H_2SO_4 (electrode area 0.144 cm^2, scan rate 20 mV/s): (a) N_2-saturated solution; (b) O_2-saturated solution.

Table III. Thin-Layer Coulometry Results of O_2 Reduction Catalyzed by $Co^{III}TMPyP$[a]

[CoTMPyP], M	pH	[O_2], mM	e^-/O_2
5.93×10^{-4}	1.8	0.24	2.05
5.93×10^{-4}	1.8	1.2	1.94
1.13×10^{-3}	7.0	0.24	2.10
1.13×10^{-3}	7.0	1.2	1.97
2.06×10^{-3}	1.8	0.24	1.94
2.06×10^{-3}	1.8	1.2	1.84
			1.97 ± 0.15 (av)

[a] Potential stepped from +0.5 to −0.2 V vs. Ag/AgCl.

The non-methylated CoTPyP shows a thiocyanate effect similar to that of CoTPyP electrochemistry in acidic solutions with K_{f_1} and K_{f_2} values of 6.3 (±0.1) × 10^3 and 13 ± 2 M^{-1}, respectively, for the formation of the mono- and bis(thiocyanato) complexes.

3. Oxygen Catalysis by CoTMPyP. A. Homogeneous Case. The CV's of $Co^{III}TMPyP$ (0.1 N H_2SO_4) in the absence and presence of oxygen are compared in Figure 5, traces a and b. There is a close correspondence between the potential for catalysis and the potential for reducing $Co^{III}TMPyP$ to the Co(II) form. The linearity of the i_{pc} vs. $v^{1/2}$ plot indicates that the total CV wave for O_2 reduction is diffusion controlled. The stoichiometry of the catalytic wave was confirmed by thin-layer coulometry to be n = 1.97 ± 0.15 for electrolysis over a considerable variation of concentrations of $Co^{III}TMPyP$, proton, and O_2. The results are summarized in Table III.

Bulk electrolyses were also conducted with solution and adsorbed $Co^{III}TMPyP$ on a GCE with continual bubbling of O_2 to assess the efficiency of H_2O_2 generation and the stability of CoTMPyP. The quantity of H_2O_2 was determined by $KMnO_4$ titration. In the case of solution $Co^{III}TMPyP$, the $Co^{III}TMPyP$ was removed prior to titration by running the solution through an ion-exchange column. The data indicated that bulk H_2O_2 could be generated with greater than 90% current efficiency. In 2 h, a 10% decrease in the $Co^{III}TMPyP$ concentration was observed, as monitored spectrally at a wavelength of 430 nm, but the conversion efficiency appeared not to be degraded. It was also noted that the efficiency decreased if the electrode potential was made more negative than −0.1 V during electrolysis.

The close correspondence between the potential for the catalysis and the redox potential of the $Co^{III/II}TMPyP$ couple suggests an "EC" type mechanism similar to that already discussed for FeTMPyP. However, in the present case if the $E_{p,cat}$ values vs. pH are plotted, as in curve b of Figure 2, the $E_{p,cat}$'s are seen to be shifted slightly negative of the reversible $E°'$ values of the $Co^{III/II}TMPyP$ couple in the pH 1–4 range. This shift results from plotting the peak of the catalytic wave rather than some value of potential near the foot of the catalytic wave, where $Co^{II}TMPyP$ begins to be generated, and the overpotential for reducing $Co^{III}TMPyP$. However, as the pH becomes more alkaline, a double wave appears for the catalysis until, at pH >4, only the

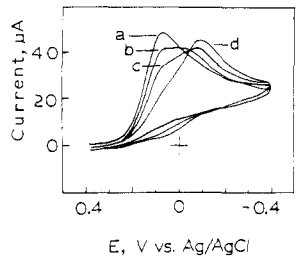

Figure 6. Cyclic voltammograms of catalytic O_2 reduction by 2.69×10^{-4} M CoTMPyP at pH 3–4 (electrode area 0.144 cm^2, scan rate 20 mV/s): (a) pH 3.0; (b) pH 3.3; (c) pH 3.6; (d) pH 4.0.

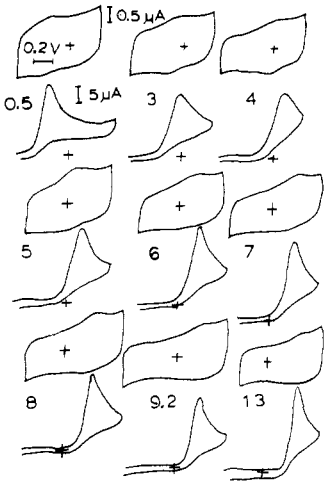

Figure 7. Cyclic voltammograms of adsorbed CoTMPyP and catalyzed O_2 reduction at various pHs.

catalytic wave at the more negative potential is seen (see CV wave vs. pH in Figure 6). The $Co^{III}TMPyP$ concentration was 2.7×10^{-4} M in these experiments with the solution air saturated (O_2 concentration ca. 0.24 mM). Such a shift in $E_{p,cat}$ is unexplained by an acid–base equilibria of the solution $Co^{III}TMPyP$ since its pK_a values are 6 and 10. In the pH 6–8 range, $E_{p,cat}$ decreased 60 mV/pH unit and then becomes nearly independent of pH at pH >8. The situation is complicated by the fact that there must necessarily be surface-adsorbed CoTMPyP when CoTMPyP is in solution. Possible explanations for the differences between the general shape of the $E_{p,cat}$ vs. pH curve to that of $E^{\circ\prime}$ vs. pH for the $Co^{III/II}TMPyP$ redox couple will be deferred until after the O_2 catalysis by surface-adsorbed $Co^{III}TMPyP$ is presented.

At pH >9, an anodic wave is observed due to the oxidation of H_2O_2 in a manner similar to that found by Durand and Anson[29] for adsorbed CoTDP. Addition of H_2O_2 to the solution enhanced this anodic peak height. However, the decomposition of CoTMPyP and H_2O_2 appeared to be much faster in the high-pH region than in acidic solutions so that further quantitation of this anodic wave was not attempted.

B. Adsorbed Case. If a GCE is exposed to a $Co^{III}TMPyP$ solution and then removed, washed with distilled water, and then immersed into an air-saturated 0.1 N H_2SO_4 solution without cobalt porphyrin present, a well-defined O_2 catalytic wave can be observed with the $E_{p,cat}$ occurring near the redox potential of the solution $Co^{III}TMPyP$. The cyclic voltammograms, in the absence and presence of oxygen, for adsorbed cobalt porphyrin are shown in Figure 7 as a function of pH. The presence of adsorbed porphyrin is more evident in the differential pulse voltammograms, as shown in Figure 8, for background (trace a) and for the GCE with adsorbed porphyrin (trace b) in the presence of oxygen. At pH 1–10, there is a close correspondence between the differential pulse voltammetric E_p values of the adsorbed porphyrin and the CV $E_{p,cat}$ values. However, a study of the potential dependence vs. pH for adsorbed cobalt porphyrin and oxygen catalysis indicates, surprisingly, that the pH dependence of the adsorbed case is considerably different from the solution

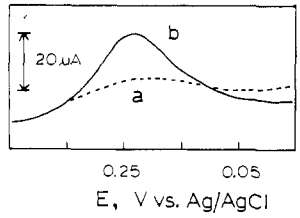

Figure 8. Differential pulse voltammograms of surface-adsorbed CoTMPyP in 0.1 N H_2SO_4 solution (electrode area 0.144 cm^2, scan rate 5 mV/s): (a) N_2 saturated; (b) O_2 saturated.

case. Thus, E_p vs. pH, plotted (trace c) in Figure 2, allows a comparison to be made with the solution case. The 60 mV/pH unit dependence to the E_p occurred at pH of ca. 2 rather than 6, as it did in the degassed-solution case. Thus, it is concluded that the *pK_{a_1} of adsorbed $Co^{III}TMPyP$ is 2.* The potential became independent of pH at ca. 8.0, which is assumed to be the pK_{a_1} of the adsorbed, *cobaltous* porphyrin.

The difference in the pH dependence of the redox potential between the solution and the adsorbed CoTMPyP suggests that, as the pH is increased, the catalysis of O_2 reduction by adsorbed CoTMPyP becomes less important when $Co^{III}TMPyP$ is present in solution. Thus, this gradual transition from a composite solution and an adsorbed CoTMPy to predominantly a solution CoTMPyP catalysis explains the CV's previously seen in Figure 6. However, a discontinuity occurs at pH ca. 4. This discontinuity is believed to arise from the fact that the formal potential of the solution $Co^{III/II}TMPyP$ becomes more positive than that of the O_2/H_2O_2 redox couple. The thermodynamics becomes unfavorable for the solution cobaltous porphyrin to reduce O_2 to H_2O_2 at pH >4. Thus, O_2 is not catalyzed until the electrode potential moves to more negative values where the adsorbed $Co^{III}TMPyP$ is reduced.

The $E_{p,cat}$ vs. pH curve (curve b, Figure 2) appears to have two inflection points at pH 6 and 8 that coincide with pK_{a_1} values of solution $Co^{III}TMPyP$ and adsorbed $Co^{II}TMPyP$, respectively. Whether the correspondence between the inflections and the pK_a values is more than coincidental is being currently investigated.

C. Effect of Thiocyanate Ion on O_2 Catalysis. Curve d of Figure 2 is a plot of $E_{p,cat}$ vs. pSCN (lower scale) when SCN^- is added to an air-saturated solution at pH 1. The O_2 is being catalyzed with CoTMPyP *adsorbed* on a glassy-carbon electrode. The $E_{p,cat}$ becomes more negative with a slope of ca. −67 mV/pSCN unit. This slope indicates that the SCN^- is dissociated from the adsorbed $Co^{II}TMPyP$ prior to the catalysis of O_2. The SCN^- dissociation is consistent with the previous results for the reduction of solution $Co^{III}TMPyP$ in the presence of SCN^-.

In the pH range of 0–4, the value of $E_{p,cat}$ will be determined by the pH and the extent to which the overpotential for $Co^{III}TMPyP$ is reduced by the presence of SCN^-, irrespective of whether we have solution or only adsorbed CoTMPyP at a glassy-carbon electrode. This favorable effect of SCN^- to shift the $E_{p,cat}$ to coincide with the $E^{\circ\prime}$ of $Co^{III/II}TMPyP$ is most pronounced, in the case of solution CoTMPyP, when there is an overpotential of ca. 100–200 mV. The SCN^- concentration should be kept relatively low so that the fractional concentration of the uncomplexed $Co^{III}TMPyP$ remains above 0.5 (refer to curves a and b of Figure 4).

The electrochemistry of CoTMPyP in alkaline solutions with SCN^- present has also been examined. For example, $Co^{III}TMPyP(H_2O)(SCN^-)$ is the principal solution species at pH 8, formed via the substitution reaction[33]

$$Co^{III}TMPyP(H_2O)(OH^-) + SCN^- + H^+ = Co^{III}TMPyP(H_2O)(SCN^-) + H_2O \quad (13)$$

with an equilibrium constant of 6.4×10^9 M^{-2}. The pK_a of mono(thiocyanato) complex is estimated to be 10. Similarly to acidic solutions, however, the uncomplexed *cobaltous* porphyrin is formed when $Co^{III}TMPyP(H_2O)(SCN^-)$ is electrochemically reduced in alkaline solutions. Thus, it becomes possible, through *judicious choice of pH and SCN^- concentration, to adjust the potential of O_2 catalysis to coincide closely with the reversible*

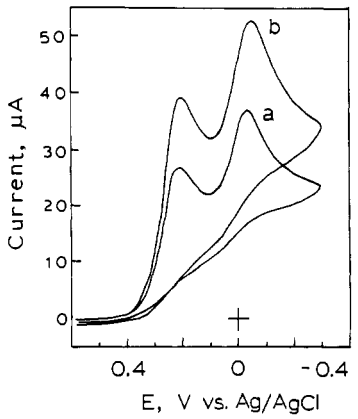

Figure 9. Cyclic voltammograms of O_2 reduction catalyzed by adsorbed CoTPyP and solution FeTMPyP in O_2-saturated 0.1 N H_2SO_4 solution (electrode area 0.124 cm^2). Scan rate: (a) 20 mV/s; (b) 40 mV/s.

potential of the O_2/H_2O_2 redox couple. For example, we have observed an $E_{p,cat}$ of −0.02 V (vs. Ag/AgCl) for O_2 reduction in a solution containing 5×10^{-4} M $Co^{III}TMPyP$ and 1×10^{-3} M SCN^- at a pH of 7.4 with a glassy-carbon electrode. Further detailed studies of this phenomenon are under way and will be reported separately.

4. Dual Catalysts: CoTMPyP and FeTMPyP. Electrogenerated $Co^{II}TMPyP$ reduces O_2 to H_2O_2 at a potential more positive than that at which $Fe^{II}TMPyP$ reduces both O_2 and H_2O_2. Hence, a double wave is observed when O_2 is reduced by an electrode with adsorbed $Co^{III}TMPyP$ in a solution containing $Fe^{III}TMPyP$ in 0.1 N H_2SO_4, as shown in Figure 9. If the adsorbed cobalt porphyrin reduced O_2 to H_2O and not H_2O_2, then the second catalytic wave would be absent. Thus, the results are consistent with H_2O_2 being produced by the cobalt porphyrin and the iron porphyrin reducing H_2O_2 to water at the second wave. The use of dual catalysts, acting in series, appears to be a promising way in which to accelerate a catalytic process[41] or to govern the products of the applied potential, as indicated in the above example.

Discussion and Conclusions

A study of the electrochemical behavior of solution and adsorbed CoTMPyP, in the absence and presence of O_2, as a function of pH has shown that the acid–base properties are considerably altered by the adsorption process. That is, the pK_{a_1} of adsorbed $Co^{III}TMPyP$ is shifted to more acidic values by ca. 4 pK_a units in comparison to the solution $Co^{III}TMPyP$. Such a large shift was unexpected, and previously unobserved for any adsorbed metal macrocycles. Although there is a possibility that the four cationic methylpyridyls, located on the periphery of the macrocyclic ring, could be involved in the adsorption, any lessening of the positive charge of these methylpyridyls would inductively affect the metal center acidity in a direction opposite to that observed. Also, it is unlikely that the acid–base properties can be influenced markedly by any changes to the methylpyridyls since the pyridine rings are perpendicularly oriented and nonconjugated (to the π electrons) to the macrocyclic ring. A possible explanation is that the metal center is interacting with the GCE surface to change the acid–base properties of the $Co^{III}TMPyP$. Inductively, an electron-withdrawing effect to the metal center is required. A possibility is that the carbon–oxygen functionalities on the surface of the GCE, such as hydroxyl, keto, and carboxylate ions, coordinate to the cobalt and thereby cause the observed effect.

In an independent study,[42] two different carbon–oxygen functionalities with $E^{\circ\prime}$ values of +0.19 and +0.25 V (vs. Ag/AgCl) on the surface of the polished GCE in acidic solutions (pH 2) have been detected with use of differential pulse voltammetry. Besides bonding interactions, these functionalities could also play a role in mediating the electron transfer to $Co^{III}TMPyP$ by virtue of the proximity of their redox potentials to that of CoTMPyP. A detailed study is currently under way to correlate the electrochemistry of the GCE surface with the behavior observed when $Co^{III}TMPyP$ is adsorbed, in an attempt to elucidate the role of such surface functionalities to the chemistry of $Co^{III/II}TMPyP$ (and CoTPyP). However, irrespective of the mechanism responsible for the pK_a shift, it is significant that it is possible to separate and delineate surface-adsorbed from solution $Co^{III}TMPyP$ catalysis of O_2 via the judicious choice of pH. Such separation is not always obvious, as has been pointed out by Shigehara and Anson.[30]

The close correspondence between the potential for catalysis and the experimental potential for the reduction of $Co^{III}TMPyP$ supported the validity of an "EC" reaction sequence. Thus, electrochemical and optically coupled experiments in thin-layer and bulk cells, often conducted under coulometric conditions, verified that oxygen was reduced to hydrogen peroxide via the electrogenerated *cobaltous* porphyrin. How closely $E_{p,cat}$ will track the $E^{\circ\prime}$ of the $Co^{III/II}TMPyP$ redox potential will depend on several factors such as (1) the overpotential for the reduction of solution or adsorbed $Co^{III}TMPyP$, (2) the pH, and (3) the rate constant for the reduction of O_2 by both the solution and adsorbed cobaltous porphyrin. The importance of these factors was nicely illustrated in the pH range of 3–5, where the solution cobaltous porphyrin no longer reduced O_2 to H_2O_2 and the potential of the catalysis shifted negatively to be governed by the potential of the adsorbed porphyrin.

The heterogeneous rate of electron transfer from GCE to bulk $Co^{III}TMPyP$ was accelerated when SCN^- was added at low concentrations (<0.1 mM) to $Co^{III}TMPyP$ solution; k_s was increased by ca. 3 orders of magnitude as the SCN^- concentration was increased. The results are consistent with the previously reported observations regarding the acceleration of the homogeneous self-exchange and of the electron-transfer rates involving cobalt porphyrins and other macrocycles.[43–48] In particular, it appears that the rates of self-exchange and electron transfer via the outer-sphere mechanism involving cobalt porphyrins[44] or cobalt macrocycles[45–48] may be slow. For example, the values of the self-exchange rate constant, k_{11}, of $Co^{III}TMPyP$ and CoTSPP were 20 and 0.061 M^{-1} s^{-1}, respectively.[40,43] These values compare to 1.2×10^6 M^{-1} s^{-1} for $Fe^{III}TMPyP$.[49] Fleischer and Chapman[44,45] also studied the self-exchange rates of cobalt porphyrins in nonaqueous solvents and found that CoTPP and CoTTP have low outer-sphere rates similar to that of the water-soluble $Co^{III}TMPyP$. In the presence of bridging ligands such as N_3^-, SCN^-, and halides, the self-exchange rates by an inner-sphere route were increased by 4–6 orders of magnitude. Pasternack et al.[36] also reported that the rates of reduction of $Co^{III}TMPyP$ by Cr^{2+} and $Ru^{II}(NH_3)_6^{2+}$ in aqueous solution were enhanced by the presence of SCN^-.

The rate enhancements for inner-sphere electron transfer have been rationalized by Endicott and co-workers[46–48] as being due to (1) a small reorganizational barrier for the inner-sphere pathway, (2) the solvent reorganizational barrier approaching zero, and (3) the inner-sphere route perhaps being somewhat adiabatic compared to the corresponding outer-sphere one. It is tempting to invoke a change from outer to inner sphere for CoTMPyP in the presence of thiocyanate ion. However, the uniqueness of SCN^- to $Co^{III}TMPyP$ redox and oxygen catalysis is the apparent rapid loss of SCN^- when the porphyrin is reduced to the cobaltous state. The extent of electron-transfer rate enhancement, in the present case, also depends on the judicious choice of system pH. It would

(41) Shigehara, K.; Anson, F. *J. Electroanal. Chem. Interfacial Electrochem.* **1982**, *132*, 107.
(42) Hu, I.-F.; Karweik, D.; Kuwana, T. *J. Electroanal. Chem. Interfacial Electrochem.* **1985**, *188*, 59.
(43) Taniguchi, V. T.; Fleischer, E. B., private communication.
(44) Chapman, R. D.; Fleischer, E. B. *J. Am. Chem. Soc.* **1982**, *104*, 1575.
(45) Chapman, R. D.; Fleischer, E. B. *J. Am. Chem. Soc.* **1982**, *104*, 1582.
(46) Kumar, K.; Rotzinger, F. P.; Endicott, J. F. *J. Am. Chem. Soc.* **1983**, *105*, 7064.
(47) Durham, B.; Endicott, J. F.; Wong, C.-L.; Rillema, D. P. *J. Am. Chem. Soc.* **1979**, *101*, 847.
(48) Rotzinger, F. P.; Kumar, K.; Endicott, J. F. *Inorg. Chem.* **1982**, *21*, 4111.
(49) Pasternack, R. F.; Spiro, E. G. *J. Am. Chem. Soc.* **1978**, *100*, 968.

be very interesting to assess the effect of pH variation and addition of SCN^- to the electrochemical and catalytic behavior of adsorbed cofacial CoP,[50-53] which appear to reduce O_2 to H_2O in an overall four-electron process.

The high conversion efficiency of O_2 to H_2O at favorable potentials by the cobalt porphyrins has served as the basis for a 200% efficient electrosynthesis cell where the cathodically generated H_2O_2 served as an effective oxidizing reagent.[28] Practical application of this, as well as other catalysts, will rely on long-term stability. Recent results on the question of catalytic stability suggested that a slow accumulation of CoP–oxygen or CoP–peroxy intermediates may be responsible for the gradual decay of activity of the adsorbed $Co^{III}TMPyP$ on the GCE. Attempts to identify such intermediates and to devise means of reactivation are currently under way and will be reported separately.

Acknowledgment. We gratefully acknowledge the financial support of this work by grants from the National Science Foundation and Koppers Company, Inc. (Pittsburgh, PA). The generous hospitality by T. Osa (Tohoku University) and K. Niki (Yokohama National University) to T.K., which allowed the writing of this paper during a professional leave, is greatly appreciated.

Registry No. $Co^{III}TMPyP$, 51329-41-0; $Co^{II}TMPyP$, 79346-65-9; $Co^{III}TMPyP(H_2O)_2$, 51405-04-0; $Co^{II}TMPyP(H_2O)_2$, 98064-63-2; $Co^{III}TMPyP(H_2O)(OH^-)$, 66114-42-9; $Co^{III}TMPy(OH^-)_2$, 98064-64-3; $Co^{III}TPyP(H_2O)_2$, 98064-65-4; $Co^{II}TPyP(H_2O)_2$, 98064-66-5; TPyP, 16834-13-2; H_2O_2, 7722-84-1; SCN^-, 302-04-5; O_2, 7782-44-7; H_2SO_4, 7664-93-9; C, 7440-44-0.

(50) Collman, J. P.; Morrocco, M.; Denisevich, P.; Koval, C.; Anson, F. *J. Electroanal. Chem. Interfacial Electrochem.* **1979**, *101*, 117.
(51) Collman, J. P.; Denisevich, P.; Konai, Y.; Morrocco, M.; Koval, C.; Anson, F. *J. Am. Chem. Soc.* **1980**, *102*, 6026.
(52) Durand, R. R., Jr.; Bencosme, C. S.; Collman, J. P.; Anson, F. *J. Am. Chem. Soc.* **1983**, *105*, 2710.
(53) Chang, C. K.; Liu, H. Y.; Abdalmuhdi, I. *J. Am. Chem. Soc.* **1984**, *106*, 2725.

Contribution from the Kenan Laboratories of Chemistry, The University of North Carolina at Chapel Hill, Chapel Hill, North Carolina 27514

Instability of the Oxidation Catalysts $[(bpy)_2(py)Ru(O)]^{2+}$ and $[(trpy)(phen)Ru(O)]^{2+}$ in Basic Solution

LEE ROECKER, WLODZIMIERZ KUTNER,† JOHN A. GILBERT, MIRIAM SIMMONS,§ ROYCE W. MURRAY, and THOMAS J. MEYER*

Received January 14, 1985

The Ru(IV) complexes $[(bpy)_2(py)Ru(O)]^{2+}$ (**1**) and $[(trpy)(phen)Ru(O)]^{2+}$ (**2**) (bpy = 2,2′-bipyridine, py = pyridine, trpy = 2,2′,2″-terpyridine, and phen = 1,10-phenanthroline) are unstable toward self-reduction in basic solution. Product analyses, performed by using UV–vis spectroscopy, cyclic voltammetry, HPLC, and GC, show that O_2 is not a product of the self-reductive chemistry and that ca. 80% of the reduced products that appear are the unmodified polypyridyl complexes of Ru(II), $[(bpy)_2(py)Ru(OH)]^+$ or $[(trpy)(phen)Ru(OH)]^+$. The remaining 20% of the products are accounted for by at least four different products, which are also Ru(II) but appear to have undergone varying degrees of ligand oxidation. Kinetic studies were performed with stopped-flow or conventional mixing techniques. For complex **2**, plots of log $|A_\infty - A_t|$ vs. time were linear from pH 12 to 14 and the experimental rate law can be described by $-d[Ru(IV)]/dt = k_a[OH^-] + k_b[OH^-]^2$, where $k_a = 0.21 \pm 0.01\ M^{-1}\ s^{-1}$ and $k_b = 0.08 \pm 0.02\ M^{-2}\ s^{-1}$ at 25 °C and $\mu = 1.0$ M (Na_2SO_4). For the k_a path $\Delta H^\ddagger = 12 \pm 2$ kcal/mol and $\Delta S^\ddagger = -20 \pm 6$ eu. For complex **1**, plots of log $|A_\infty - A_t|$ vs. time were not linear but could be resolved into two successive components to yield rate constants for the self-reduction of Ru(IV) and, following that, of Ru(III). The differences in behavior in basic media between complexes **1** and **2**, and possible mechanistic schemes for the self-reduction, are discussed as are possible implications of the ligand-based redox chemistry for utilization of the ruthenium oxo complexes as oxidation catalysts in basic solution.

Polypyridyl complexes containing the $Ru^{IV}{=}O$ group have been observed to act as stoichiometric or catalytic oxidants for a variety of organic and inorganic substrates.[1-9] A potentially important variable in using these reagents as oxidants is pH. For example, while acetone is virtually unreactive toward $[(trpy)(phen)Ru(O)]^{2+}$ in acidic solution ($k < 10^{-6}\ M^{-1}\ s^{-1}$ at pH 2), oxidation of acetone is rapid in basic solution ($k = 8.75\ M^{-1}\ s^{-1}$ at pH 13).[9]

Although aquo or hydroxo polypyridyl complexes of Ru(II) are stable at any pH, higher oxidation states are somewhat unstable in basic media toward self-reduction to Ru(II). Ghosh et al.[10] have noted that the instability of $[Ru(bpy)_3]^{3+}$ toward spontaneous reduction in basic solution occurs, at least in the first stage, by oxidative hydroxylation of the polypyridyl ligands. Nord, et al.[11] have proposed that the spontaneous decay of Fe(III) polypyridyl complexes leads to Fe(II) complexes and coordinated, ligand-based *N*-oxides as primary products.

We have investigated and report here the results of a series of studies on the instabilities of $[(trpy)(phen)Ru(O)]^{2+}$ and $[(bpy)_2(py)Ru(O)]^{2+}$ in basic solution toward self-reduction. It is an important study from our point of view because the possibility of developing selective functional group oxidation schemes based on Ru–oxo complexes depends, in part, on an ability to utilize pH variations, and therefore, it is necessary to define the pH regions of catalyst stability.

Experimental Section

Materials. Reagent grade $(NH_4)_2[Ce(NO_3)_6]$ (G. F. Smith Chemical Co.) was used to prepare solutions of Ce(IV), which were standardized spectrophotometrically at 320 nm ($\epsilon = 1320\ M^{-1}\ cm^{-1}$). 2-Hydroxypyridine and 1,10-phenanthroline (Aldrich Chemical Co.) were used without further purification. The electrolyte, $[(C_2H_5)_4N](ClO_4)$(TEAP), used in electrochemical measurements was recrystallized twice from H_2O

† On leave from the Institute of Physical Chemistry, Polish Academy of Sciences, 01-224 Warsaw, Poland.
§ Present address: Technology Enterprises Division/3M, 219-1-01 3M Center, St. Paul, MN 55144.

(1) Meyer, T. J. *J. Electrochem. Soc.* **1984**, *131*, 221C.
(2) Samuels, G. J.; Meyer, T. J. *J. Am. Chem. Soc.* **1981**, *103*, 307.
(3) McHatton, R. C.; Anson, F. C. *Inorg. Chem.* **1984**, *23*, 3935.
(4) (a) Thompson, M. S.; De Giovani, W. F.; Moyer, B. A.; Meyer, T. J. *J. Org. Chem.* **1984**, *49*, 4972. (b) Moyer, B. A.; Thompson, M. S.; Meyer, T. J. *J. Am. Chem. Soc.* **1980**, *102*, 2310.
(5) Thompson, M. S.; Meyer, T. J. *J. Am. Chem. Soc.* **1981**, *103*, 5070.
(6) Thompson, M. S.; Meyer, T. J. *J. Am. Chem. Soc.* **1982**, *104*, 4106.
(7) Kutner, W.; Meyer, T. J.; Murray, R. W. *J. Electroanal. Chem. Interfacial Electrochem.*, in press.
(8) Roecker, L.; Meyer, T. J., submitted for publication.
(9) Roecker, L.; Kutner, W., unpublished results.
(10) Ghosh, P. K.; Brunschwig, B. S.; Chou, M.; Creutz, C.; Sutin, N. *J. Am. Chem. Soc.* **1984**, *106*, 4772.
(11) Nord, G.; Pedersen, B.; Bjergbakke, E. *J. Am. Chem. Soc.* **1983**, *105*, 1913.

0020-1669/85/1324-3784$01.50/0